Superconductivity and crystalline electric field effects in the filled skutterudite $PrRu_4As_{12}$

T. A. Sayles, R. E. Baumbach, W. M. Yuhasz, and M. B. Maple
Department of Physics, University of California–San Diego, La Jolla, California 92093, USA

Ł. Bochenek, R. Wawryk, T. Cichorek, A. Pietraszko, and Z. Henkie
Institute of Low Temperature and Structure Research, Polish Academy of Sciences, 50-950 Wrocław, Poland

P.-C. Ho
Department of Physics, California State University, Fresno, Fresno, California 93740, USA
(Received 24 September 2009; revised manuscript received 18 May 2010; published 17 September 2010)

Magnetization, electrical-resistivity, specific-heat, and thermopower measurements were performed on single crystals of the filled skutterudite compound $PrRu_4As_{12}$. These measurements reveal a superconducting transition near 2.5 K that is quantified by: (1) magnetic susceptibility data which display an onset to a Meissner state at $T_c \approx 2.5$ K and complete diamagnetic shielding as $T \rightarrow 2.0$ K, (2) electrical-resistivity data which show a transition to a zero-resistance state at $T_c \approx 2.5$ K, and (3) specific-heat and thermopower data which display "jumps" at $T_c \approx 2.5$ K. Furthermore, the electronic contribution to the specific heat follows the BCS prediction for a superconductor. For temperatures above T_c, magnetization measurements indicate local moment behavior where $\mu_{eff}=3.52\ \mu_B/Pr^{3+}$ ion. Analysis of the data for $T>T_c$, using a crystalline electric field model, suggests that $PrRu_4As_{12}$ has a Γ_1 ground state with a Γ_4 first excited state at $T_{\Gamma_4} \approx 95$ K.

DOI: 10.1103/PhysRevB.82.104513 PACS number(s): 74.70.−b, 74.25.Bt, 74.25.F−, 74.25.Ha

I. INTRODUCTION

The family of filled skutterudite compounds with the chemical formula MT_4X_{12}—where M is an alkali metal, alkaline earth, lanthanide, or actinide; T is Fe, Ru, or Os; and X is P, As, or Sb—display a wide variety of strongly correlated electron phenomena: e.g., superconductivity (both conventional and unconventional), magnetic and quadrupolar order, metal-insulator transitions, Kondo phenomena, heavy-fermion, and non-Fermi-liquid behavior.[1–5] The Pr-based filled skutterudites provide a particularly large reservoir of interesting phenomena as a result of the interplay between several factors including: (1) hybridization between conduction electron and Pr localized f-electron states, (2) splitting of the Pr^{3+} ion Hund's rule ground-state multiplet by crystalline electric fields (CEFs), and (3) complicated electronic band structures.

To date, much of the research on the Pr-based filled skutterudite compounds has focused on those that include Sb and P, in part because of technical difficulties in synthesizing single crystals of As-based filled skutterudites. These problems were recently overcome[6] and several members of the arsenide series have now been studied in single-crystal form. Presented here are the first measurements on single crystals of the compound $PrRu_4As_{12}$. We report results for magnetization $M(T)$, specific heat $C(T,H)$, electrical resistivity $\rho(T)$, and thermopower $S(T)$, all of which show that $PrRu_4As_{12}$ displays conventional superconductivity below a critical temperature of $T_c \approx 2.5$ K. Analysis of CEF effects on $M(T)$, $C(T)$, and $\rho(T)$ are used to determine the CEF splittings of the Pr^{3+} Hund's rule multiplet.

II. EXPERIMENTAL DETAILS

Single crystals of $PrRu_4As_{12}$ were grown from elements with purities >99.9% in a molten Cd:As flux at high temperatures and pressures using a technique detailed elsewhere.[6] Following the growth, $PrRu_4As_{12}$ single crystals of an isometric form with dimensions up to ~1.0 mm were collected and etched in HCl acid to remove any impurity phases from the surfaces. X-ray powder-diffraction measurements were performed using a Rigaku D/MAX B x-ray machine on a powder that was prepared by grinding several single crystals along with a high purity Si (8N) standard. These measurements did not reveal any significant impurity phases. The $LaFe_4P_{12}$-type filled skutterudite crystal structure was confirmed for $PrRu_4As_{12}$ by x-ray diffraction on a crystal with a regular octahedral shape and dimensions of $0.21 \times 0.19 \times 0.18$ mm^3. A total of 3136 reflections (366 unique, $R_{int}=0.1018$) were recorded and the structure was resolved by the full matrix least-squares method using the SHELX-97 program with a final discrepancy factor $R1=0.0324$ [for $I>2\sigma(I)$, $wR2=0.0715$].[7,8] The refinement revealed a lattice parameter of $a=8.508(2)$ Å as well as full occupancy of the Pr sites.

Magnetization measurements were performed on single crystals of $PrRu_4As_{12}$ using a Quantum Design (QD) magnetic properties measurement system for $1.7 \leq T \leq 300$ K and $H=1$ and 50 mT. The specific heat for a collection of single crystals was measured for 600 mK$\leq T<40$ K in a ^{3}He semiadiabatic calorimeter using a standard heat pulse technique. Specific-heat measurements for $0<H<0.7$ T and $0.37<T<7$ K were performed for a different group of crystals with a total mass $m=13.4$ mg in a QD physical properties measurement system using a standard heat pulse technique. The electrical resistivity was measured for $2 \leq T \leq 300$ K for a single-crystal specimen in a ^{4}He cryostat using an ac resistance bridge and a standard four-wire technique. Measurements of the thermoelectric power for $0.5<T<350$ K were performed on single crystals with lengths less than 1 mm using a method described by Wawryk and Henkie.[9]

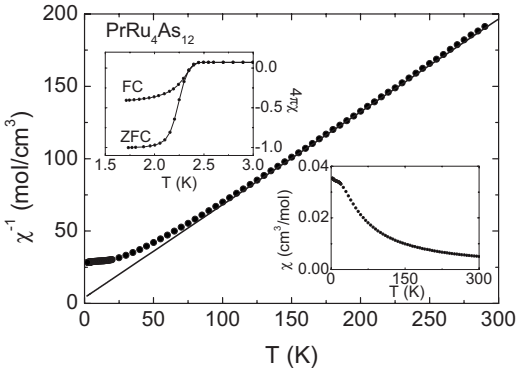

FIG. 1. Inverse magnetic susceptibility χ^{-1} vs temperature T in a 50 mT field. The solid line is a Curie-Weiss fit to the data for $115 \leq T \leq 300$ K. Left inset: zero-field-cooled (ZFC) and FC volume magnetic susceptibility $4\pi\chi$ vs T data for $PrRu_4As_{12}$ in a 1 mT field. The ZFC data display perfect diamagnetism at $T \approx 2$ K where $4\pi\chi \rightarrow -1$ due to the diamagnetic shielding signal, while the FC data show the development of a Meissner state at $T_c \approx 2.5$ K. Right inset: magnetic susceptibility $\chi = M/H$ vs T in a 50 mT field.

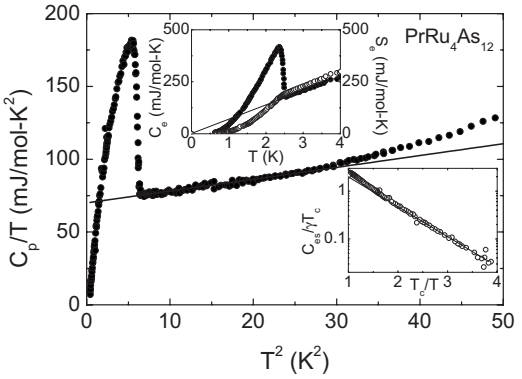

FIG. 2. Specific heat divided by temperature C_p/T vs T^2 for $PrRu_4As_{12}$ showing the transition from the normal state to the superconducting state at $T_c \approx 2.5$ K. The solid line shows $\gamma T + \beta T^3$ for $3 \leq T \leq 5$ K where the Sommerfeld coefficient $\gamma \approx 70$ mJ/mol K^2 and $\beta = 0.813$ mJ/mol K^4, from which the Debye temperature $\theta_D = 344$ K is calculated. Left inset: low-temperature electronic contribution to the specific heat C_e (closed circles) and entropy (open circles) S_e for $PrRu_4As_{12}$. The solid line is the normal-state entropy S_{ne} extrapolated from $T_c \approx 2.5$ K $< T$ assuming Fermi-liquid behavior. Right inset: electronic contribution to the specific heat in the superconducting state plotted as $C_{es}/\gamma T_c$ vs T_c/T on a semilogarithmic plot. The solid line represents a fit to the data using Eq. (1) where $A = 8.4$ and $B = 1.44$.

III. RESULTS

A. Magnetization

Magnetic susceptibility $\chi = M/H$ vs T measurements were performed for two single crystals of $PrRu_4As_{12}$ in fields of 1 and 50 mT (oriented along the [100] crystallographic axis). As shown in Fig. 1, $\chi(T)$ for $H = 50$ mT can be fitted using a Curie-Weiss (CW) function $\chi(T) = C/(T - \theta_{CW})$ for temperatures between 115 and 300 K, yielding a Curie-Weiss temperature $\theta_{CW} = -6.21$ K and an effective magnetic moment $\mu_{eff} = 3.52\ \mu_B$ (in close agreement with the Pr^{3+} free ion value of 3.58 μ_B). Below 100 K, the data deviate from CW behavior, indicating that CEF splitting becomes important at lower T. The left inset of Fig. 1 displays the low-temperature zero-field-cooled (ZFC) and FC volume magnetic susceptibilities for $H = 1$ mT, revealing the onset of superconductivity at $T_c \approx 2.5$ K. The ZFC measurement shows that $\chi(T) \rightarrow \frac{-1}{4\pi}$ for $T \lesssim 2$ K, indicating complete diamagnetic shielding. The FC data show 40% of the full Meissner state for $T \leq 2$ K, which provides evidence for the formation of a bulk superconducting state.

B. Specific heat

Displayed in Fig. 2 are specific heat C_p divided by T vs T^2 data for $PrRu_4As_{12}$ between 0.6 and 7 K. A linear fit to the data in the region above the superconducting transition using the function $C_p/T = \gamma + \beta T^2$ (for $3 \leq T \leq 5$ K) yields the Sommerfeld coefficient $\gamma \approx 70$ mJ/mol K^2 and $\beta = 0.813$ mJ/mol K^4, from which the Debye temperature $\theta_D = 344$ K is calculated. The superconducting transition is sharp, indicating good sample homogeneity. The jump in C_p/T begins near 2.5 K and an equal area construction gives $T_c \approx 2.44$ K, in good agreement with the values found from $\rho(T)$ and $\chi(T)$ data.

To investigate the nature of the superconducting state, fits of the electronic specific heat $C_{es} = C_p - C_l$, where C_l is the lattice portion of the specific heat determined from the linear fit described above, were made below T_c. For conventional superconductors, $C_{es}(T)$ can be fit by an exponential BCS function, as is appropriate for an isotropic energy gap, while for unconventional superconductors, $C_{es}(T)$ can often be described by a power law that is attributed to nodes in the energy gap. $C_{es}(T)$ for $PrRu_4As_{12}$ is described by an exponential function for $T \leq 0.6T_c$, indicative of conventional superconductivity with an isotropic energy gap. A semilogarithmic plot of $C_{es}/\gamma T_c$ vs T_c/T is shown in the right inset of Fig. 2 along with a fit to the equation,

$$\frac{C_{es}}{\gamma T_c} = A \exp\frac{-BT_c}{T}, \tag{1}$$

where A and B are fitting parameters. In the region $2.5 < T_c/T < 4$, the fit yields $A = 8.4$ and $B = 1.44$, in very close agreement with the predictions given by the BCS theory.

The jump in the specific heat near the superconducting transition, $\Delta C(T_c)$, provides information about the strength of the coupling. For $PrRu_4As_{12}$, $\Delta C(T_c)/\gamma T_c = 1.53$, which is close to the weak-coupling prediction $[\Delta C(T_c)/\gamma T_c = 1.43]$ for a BCS superconductor. This value is quite different than the value of $\Delta C(T_c)/\gamma T_c = 0.83$ found by Namiki[10] for a polycrystalline specimen of $PrRu_4As_{12}$, suggesting that the single crystals are of higher quality.

Also shown in the left inset of Fig. 2 are the electronic portion of the entropy S_e and C_e vs T for $PrRu_4As_{12}$. As expected, the superconducting state entropy S_{se} is less than that of the normal-state entropy S_{ne} since the superconducting state is more ordered. We also observe that $C_e < S_e$ for $T_c < T$, in contrast to what is expected for a Fermi liquid. Although we cannot make any definitive statement, since measurement error could yield this difference, we note that

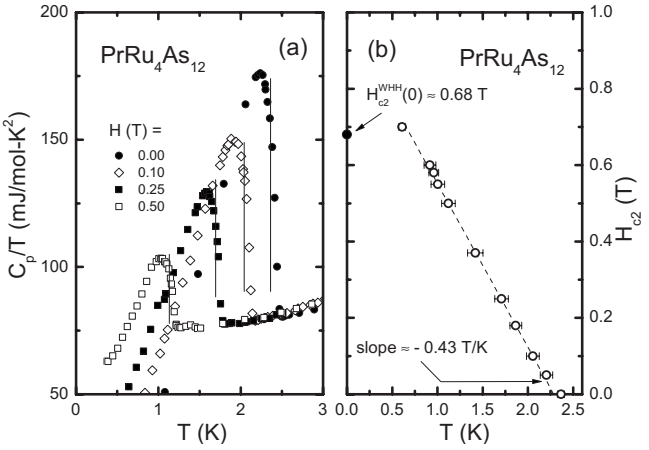

FIG. 3. (a) Specific-heat data for $0<H<0.7$ T and $0.37<T<3$ K. The superconducting critical temperature T_c is determined using an equal entropy construction which is represented by the straight lines. (b) The temperature dependence of the upper critical field $H_{c2}(T)$.

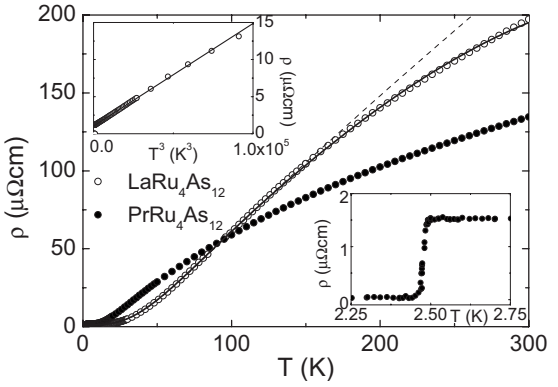

FIG. 4. Open circles: electrical resistivity ρ vs temperature T for $LaRu_4As_{12}$. Closed circles: $\rho(T)$ for $PrRu_4As_{12}$. Dashed line: fit to $\rho(T)$ for $LaRu_4As_{12}$ using Eq. (3). Solid line: fit to $\rho(T)$ for $LaRu_4As_{12}$ using Eq. (3) with an additional term BT^3. Left inset: ρ vs T^3 for $LaRu_4As_{12}$ showing that $n=3$ for the Bloch-Grüneisen formula. Right inset: ρ vs T for $PrRu_4As_{12}$ showing that $T_c \approx 2.5$ K.

this situation could arise if C_e were to deviate from T-linear behavior for $T<T_c$.

Specific-heat measurements were performed for $0<H<0.7$ T and $0.37<T<3$ K [Fig. 3(a)]. From these data, the temperature dependence of the upper critical field $H_{c2}(T)$ [Fig. 3(b)] was determined using an equal entropy construction. Disregarding the small positive curvature near T_c, the initial slope $(-dH_{c2}/dT)_{T_c}$ is 0.43 T/K and is 20% larger than that previously reported for polycrystalline samples.[10] The Pauli paramagnetic limiting field can be calculated from the expression $H_{p_0}(0)=1.84T_c$ which gives a value near 4.4 T.[11,12] By comparison, the Werthamer-Hefland-Hohemberg (WHH) formula for the orbital critical field in the clean limit yields $H_{\mathrm{WHH}}(0)\simeq 0.71$ T.[13] Thus, we conclude that the superconductivity is limited by orbital depairing mechanisms.

The superconducting coherence length can be determined from the expression $(-dH_{c2}/dT)_{T_c}=\Phi/2T_c\pi\xi_0^2$, yielding $\xi_0=178$ Å.[14] The Fermi velocity $v_F=3.1\times10^6$ cm/s can then be calculated from the expression $\xi_0=0.18\hbar v_F/k_BT_c$.[15] From v_F, the charge carrier effective mass m^* and the coefficient of the electronic specific heat γ can be estimated using a spherical Fermi-surface approximation where $k_F=(3\pi^2Z/\Omega)$. Here, Z is the number of electrons per unit cell, and Ω is the unit-cell volume. From this expression, k_F is found to be 6.6×10^7 cm^{-1} and $m^*=\hbar k_F/v_F$ then gives $m^*=24m_e$. Finally, the electronic coefficient of the specific heat is given by $\gamma=\pi^2(Z/\Omega)k_B^2m^*/\hbar k_F^2$ and is found to be near 156 mJ/mol K^2. This value is somewhat enhanced in comparison to the value estimated from the normal-state specific heat and $\Delta C(T_c)$ at T_c. It is interesting to note that similar results were obtained for the compound $PrRu_4Sb_{12}$ where $m^*\sim24m_e$ and $\gamma\sim182$ mJ/mol K^2, as calculated using the formalism described above.[16] In that case, the extrapolated normal state values for γ and $\Delta C(T_c)$ are 75 mJ/mol K^2 and 96 mJ/mol K^2, respectively.[17]

C. Electrical resistivity

Figure 4 shows the temperature dependence of the electrical resistivity $\rho(T)$ for a single crystal of $PrRu_4As_{12}$ (closed circles). With decreasing T, $\rho(T)$ decreases from the room-temperature value $[\rho(300\ \mathrm{K})=135\ \mu\Omega\ \mathrm{cm}]$ with negative curvature down to $T\sim50$ K, after which $\rho(T)$ exhibits positive curvature down to $\rho_0=1.04\ \mu\Omega$ cm just before it drops to zero below $T_c\approx2.5$ K due to the superconducting transition (right inset of Fig. 4). From this value of ρ_0, we estimate the residual resistivity ratio RRR $=\rho(300\ \mathrm{K})/\rho_0\approx94$, which is comparable to the values found for $PrOs_4As_{12}$ and $PrFe_4As_{12}$ (RRR$\approx$75)

To analyze the electrical transport behavior for $PrRu_4As_{12}$ above T_c, we measured $\rho(T)$ for a single-crystal specimen of $LaRu_4As_{12}$ $[\rho(300\ \mathrm{K})=197\ \mu\Omega\ \mathrm{cm}]$, which is the homologous compound without f electrons (open circles in Fig. 4) to $PrRu_4As_{12}$. In order to describe $\rho(T)$ for $LaRu_4As_{12}$, we considered the following scattering processes: (1) a T-independent term ρ_0 which arises from impurities and/or defects that perturb the periodicity of the lattice potential and (2) electron-phonon scattering due to lattice vibrations, which can be described by the Bloch-Grüneisen (BG) formula,

$$\rho_{\mathrm{BG}}(T)=A\left(\frac{T}{\theta_R}\right)^n\int_0^{\theta_R/T}\frac{x^n dx}{(e^x-1)(1-e^{-x})}, \qquad (2)$$

where $n=5$ (in the original treatment) and θ_R is the Debye temperature. At low temperatures $(T<\frac{1}{8}\theta_R)$, this expression reduces to AT^5 while at high temperatures $(\frac{1}{2}\theta_R<T)$ it becomes linear in T.[18] However, the BG expression where $n=5$ is not generally valid and values of $2<n<5$ are commonly observed in intermetallic compounds with rare-earth elements.[19] For $LaRu_4As_{12}$, we find that for $10<T<39$ K, $n=3$, as shown in the left inset of Fig. 4. The $\rho(T)$ data in Fig. 4 are described well for $10<T<150$ K by the expression,

$$\rho(T)=\rho_0+A\left(\frac{T}{\theta_R}\right)^n\int_0^{\theta_R/T}\frac{x^n dx}{(e^x-1)(1-e^{-x})}, \qquad (3)$$

where $n=3$, $\rho_0=1.04\ \mu\Omega$ cm, $\theta_R=272$ K, and $A=207.3\ \mu\Omega$ cm. From this value of ρ_0, we estimate RRR

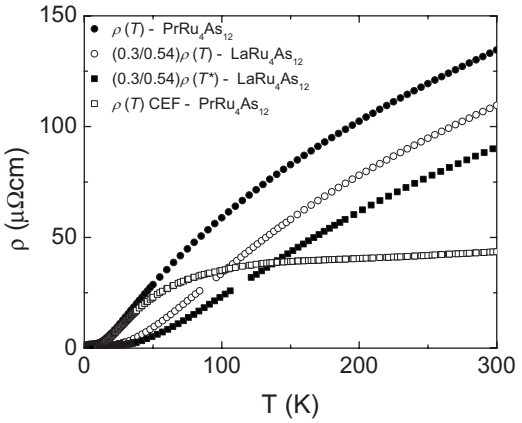

FIG. 5. Closed circles: electrical resistivity ρ vs temperature T for $PrRu_4As_{12}$. Open circles: $\rho(T)$ for $LaRu_4As_{12}$ multiplied by the constant 0.3/0.54. Closed squares: $\rho(T)$ for $LaRu_4As_{12}$ multiplied by the constant 0.3/0.54 with T scaled by the ratio $\theta_D/\theta_R = 344/272$. Open squares: the CEF contribution to $PrRu_4As_{12}$ as obtained by the procedure described in the text.

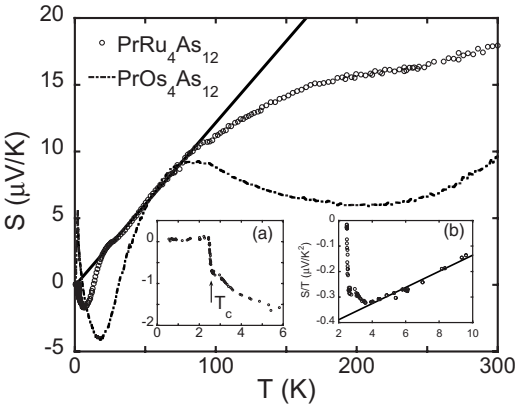

FIG. 6. Thermoelectric power S vs temperature T for $PrRu_4As_{12}$ (open circles) and $PrOs_4As_{12}$ (dashed line) with a linear fit over the region 30–75 K for the $PrRu_4As_{12}$ data. A clear difference is seen in the curvature of the data for the two compounds with convex and concave T dependence for $PrOs_4As_{12}$ and $PrRu_4As_{12}$, respectively. For $PrRu_4As_{12}$, $S(T)$ indicates possible two-band character. Left inset: the transition to the superconducting state at $T_c \approx 2.5$ K and the superconducting region where $S=0$ μV/K. Right inset: S/T vs T showing a linear extrapolation to $T=0$.

$=198$, which is a factor of two larger than found for $PrRu_4As_{12}$. Finally, we find that the data can be fitted over the entire temperature range $10<T<300$ K (solid line Fig. 4) by including a term BT^3, where $B=-1.66\times10^{-6}$ $\mu\Omega$ cm/K^3. This term is ascribed to s-d-type scattering, originally proposed by Mott, where s electrons are scattered by phonons into overlapping and incompletely filled bands. In this scenario, there is high probability that the s electrons will scatter into the dense empty states near the Fermi level associated with the d bands rather than back into the s band.[20]

Based on this treatment of $\rho(T)$ for $LaRu_4As_{12}$, we are able to deduce the contribution to $\rho(T)$ for $PrRu_4As_{12}$ without f electrons in the following way. We first normalize $\rho(T)$ for $LaRu_4As_{12}$ such that it has the same slope at high T as $\rho(T)$ for $LaRu_4As_{12}$. This is done by multiplying $\rho(T)$ for $LaRu_4As_{12}$ by 0.3/0.54 (open circles Fig. 5). Subsequently, we account for the difference between the Debye temperatures for $LaRu_4As_{12}$ and $PrRu_4As_{12}$ by multiplying the temperature scale by the ratio $\theta_D/\theta_R=344/272$, where θ_D is taken from the fit to the specific heat for $PrRu_4As_{12}$ (closed squares Fig. 5). If this modified curve is then subtracted from $\rho(T)$ for $PrRu_4As_{12}$ and $\rho_0=1.04$ $\mu\Omega$ cm (for $LaRu_4As_{12}$) is replaced by $\rho_0=1.44$ $\mu\Omega$ cm (for $PrRu_4As_{12}$), we then obtain the approximate CEF contribution to $\rho(T)$ for $PrRu_4As_{12}$ (open squares in Fig. 5).

D. Thermoelectric power

Thermoelectric power $S(T)$ data for $PrRu_4As_{12}$ along the [100] crystallographic axis are shown as open circles in Fig. 6. The $S(T)$ data for $PrRu_4As_{12}$ deviate from a straight line $S(T)=aT$ ($a=0.12$ μV/K^2) above $\sim$80 K, as expected for diffusive thermoelectric power in a single band metal. However, the negative curvature at higher temperatures may indicate that $PrRu_4As_{12}$ is a two-band metallic conductor,[21] as $S(300\ \text{K})$ only reaches 18.0 μV/K, while the resistivity is moderately low $\rho(300\ \text{K})=135$ $\mu\Omega$ cm. Additionally, a weak maximum is seen at $T\sim26$ K followed by a minimum at $T\sim11$ K. We note that a simple change in transition metal ion—Os for Ru—drastically changes $S(T)$ above $\approx$100 K.

Figure 7 shows the temperature derivative of the thermoelectric power dS/dT vs log T for $PrRu_4As_{12}$ and $PrOs_4As_{12}$. This result emphasizes the sharpness of the change in curvature and accentuates the local maxima and minima of the curves. The abrupt slope changes are defined as T_1' and T_2' and mark characteristic temperatures for electron scattering. From the plot, a great deal of similarity between the dS/dT vs log T behavior for $PrRu_4As_{12}$ and $PrOs_4As_{12}$ is evident, although the features of $PrOs_4As_{12}$ are shifted to higher T. This similarity suggests comparable mechanisms for the thermoelectric power in the two compounds.

Behnia *et al.* argue that, in the zero-T limit, the thermoelectric power should obey the relation

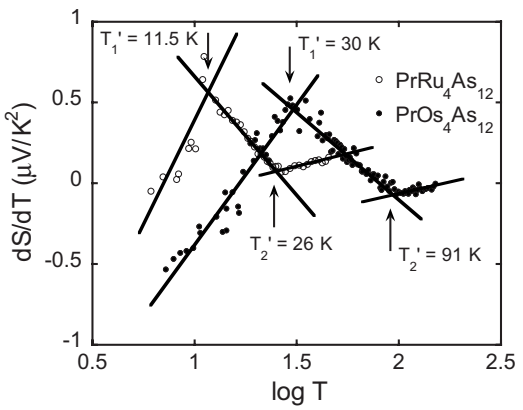

FIG. 7. Temperature derivative of the thermoelectric power dS/dT vs log T of $PrRu_4As_{12}$ along the [100] direction, compared to that of $PrOs_4As_{12}$.

$$q = (S/T)(N_A e/\gamma), \tag{4}$$

where γ is the electronic specific-heat coefficient, N_A is Avogadro's number, e is the electron charge, and the product $N_A e = 9.65 \times 10^4$ C/mol is the Faraday number.[22] The dimensionless quantity q corresponds to the density of carriers per formula unit for the case of a free-electron gas with an energy-independent relaxation time. [Equation (4) was more rigorously derived by Zlatić *et al.*[23]] Shown in inset (b) of Fig. 6 is $S(T)/T$ for $PrRu_4As_{12}$ along with a linear fit of the data over the temperature range $3.6 \leq T \leq 10$ K. As can be seen, the data are nearly linear in this region, with a minimum in $(S/T)_{min} = 0.32$ μV/K^2 before the onset of superconductivity. If the fit in the linear region is extrapolated to $T = 0$ K, then $(S/T)_{ext} \approx 0.39$ μV/K^2. Using these values [$(S/T)_{min}$ and $(S/T)_{ext}$] as well as $\gamma = 70$ mJ/mol K^2, the dimensionless quantity q is calculated to be $q \approx 0.43$ and $q \approx 0.53$, respectively; both of which are consistent with the metallic conductivity of $PrRu_4As_{12}$.

E. Crystalline electric field

In order to analyze the influence of the CEF on the Pr^{3+} ion energy levels in $PrRu_4As_{12}$, the $\chi(T)$, $\rho(T)$, and $C(T)$ data were compared to various CEF level models. In the Steven's operator formalism, the CEF Hamiltonians for cubic O_h (Ref. 24) and tetrahedral T_h symmetry[25] are

$$H_{O_h} = B_4(O_4^0 + 5O_4^4) + B_6(O_6^0 - 21O_6^4) \tag{5}$$

and

$$H_{T_h} = H_{O_h} + B_6'(O_6^2 - O_6^6), \tag{6}$$

respectively. Both groups have the same level degeneracies, although different labels and selection rules apply. While the extra term used for T_h symmetry has little effect on the actual CEF energies, it does mix the Γ_4 and Γ_5 wave functions from the O_h symmetry.[26] The difference this causes for the type of analysis to follow is small. Thus, although the true symmetry of the Pr^{3+} ion in $PrRu_4As_{12}$ is T_h, the CEF analysis employed here will use the O_h symmetry and notation.

For cubic O_h symmetry, the ninefold $J=4$ Hund's rule multiplet of Pr^{3+} is split into a Γ_1 singlet, a Γ_3 nonmagnetic doublet, and Γ_4 and Γ_5 triplets. Using the Lea, Leask, and Wolf (LLW) formalism,[24] x and W, where x is the ratio of the fourth- and sixth-order terms of the CEF Hamiltonian, and W sets the appropriate energy scale, serve as parameters to describe the energy levels.

Figure 8 shows the CEF fits to $\chi(T)$ and $\chi^{-1}(T)$ for $T = 2-300$ K in the LLW formalism where $x = 0.95$, $W = -10.4$ K, and the Landé g-factor $g = 0.8$ with energy levels Γ_1 (0 K), Γ_4 (95 K), Γ_3 (162 K), and Γ_5 (502 K). Although the low-temperature behavior is not perfectly reproduced by the CEF fit (possibly because of a small concentration of paramagnetic impurities), these parameters were found to give the best representation of the data. For this reason, we conclude that this is the most likely energy-level arrangement.

A fit to the CEF contribution to the electrical resistivity $\rho_{CEF}(T)$, where $\rho_{CEF}(T)$ was acquired using the method described in Sec. III C, is shown in Fig. 9. The fit was performed using only a magnetic exchange term for Pr^{3+} ions in a cubic environment[27] and by assuming that the CEF splitting scheme found from the fit to $\chi(T)$ accurately described the data, i.e., $x = 0.95$, $W = -10.4$ K, and the Landé g-factor $g = 0.8$ with energy levels Γ_1 (0 K), Γ_4 (95 K), Γ_3 (162 K), and Γ_5 (502 K). Since the addition of an aspherical Coulomb scattering term did not improve the quality of the fits to the $\rho_{CEF}(T)$ data for $PrRu_4As_{12}$, this contribution was not included in the analysis.

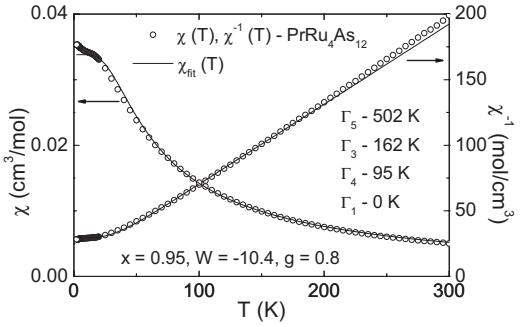

FIG. 8. Open circles: magnetic susceptibility χ and inverse magnetic susceptibility χ^{-1} vs temperature T for $PrRu_4As_{12}$ measured in a 50 mT field. Solid lines: CEF fits to the data. The LLW parameters (x and W) and the energy-level splittings are displayed in the plot.

In order to describe the total specific heat $C_p(T)$, we found that, in addition to the electronic $C_e = \gamma T$, Debye C_D, and CEF C_{CEF} components, it is necessary to include an Einstein mode lattice contribution which may arise as the result of the "rattling" motion of the Pr filler ions, as was found to be the case for several other filled skutterudites [e.g., $Tl_{0.22}Co_4Sb_{12}$ (Ref. 28) and $NdOs_4Sb_{12}$ (Ref. 29)]. To obtain an estimate of the Einstein temperature, we first considered the expression

$$U = \frac{\hbar^2}{2m_{Pr}k_B\theta_E}\coth\frac{\theta_E}{2T}, \tag{7}$$

where $U = 0.013$ Å^2 is the room-temperature thermal displacement parameter determined from single-crystal x-ray diffraction measurements,[6] m_{Pr} is the atomic mass of Pr, and

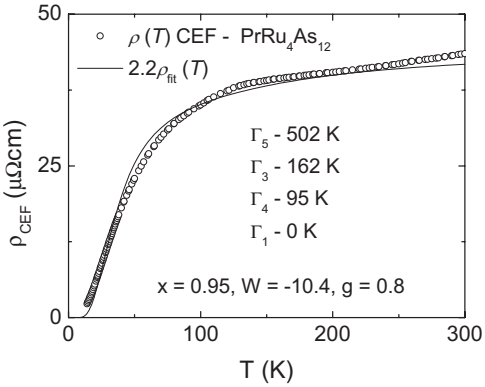

FIG. 9. Open circles: CEF contribution to the electrical resistivity ρ_{CEF} vs temperature T for $PrRu_4As_{12}$, obtained as described in the text. Solid line: CEF fit to $\rho_{CEF}(T)$. The LLW parameters (x and W) and the energy-level splittings are displayed in the plot.

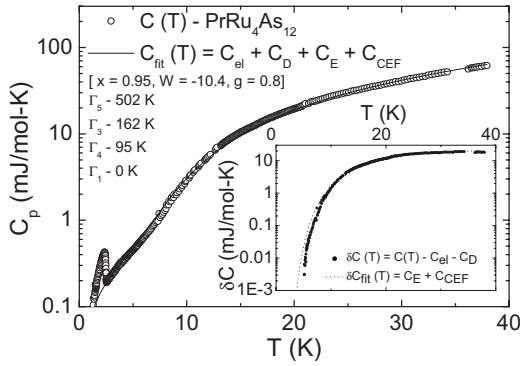

FIG. 10. Open circles: specific-heat C vs temperature T for $PrRu_4As_{12}$ on a semilogarithmic plot. Solid line: fit to $C(T)$ including the electronic C_e and CEF C_{CEF} terms in addition to the lattice terms arising from a typical phonon spectrum C_D and an Einstein rattler C_E. Inset: solid circles: $\delta C = C(T) - C_e(T) - C_D(T)$. Dotted line: fit to δC using the CEF contribution C_{CEF} and the Einstein contribution C_E.

θ_E is the Einstein temperature. From this analysis, we find that $\theta_E \approx 89$ K. Therefore, we assume that the Pr atoms partially act like Einstein oscillators with a mixing ratio r, and the lattice contribution to the specific heat can be expressed as $C_{lat} = C_E + C_D$ given by

$$C_D = (17 - r)9R\left(\frac{T}{\theta_D}\right)^3 \int_0^{\theta_D/T} \frac{x^4 e^x}{(e^x - 1)^2} dx \tag{8}$$

and

$$C_E = r\left[\frac{3R(\theta_E/T)^2 e^{\theta_E/T}}{(e^{\theta_E/T} - 1)^2}\right], \tag{9}$$

where R is the universal gas constant, θ_D is the Debye temperature, and θ_E is the Einstein temperature. If we assume that $\theta_D = 344$ K, $\gamma = 70$ mJ/mol K^2, and the CEF contribution to $C(T)$ can be calculated from the parameters described above for $\chi(T)$ and $\rho(T)$, then it is possible to adjust r and θ_E in order to optimize the fit to the data $C_{fit} = C_e + C_D + C_E + C_{CEF}$ (Fig. 10). From this analysis, we find that $r \approx 0.45$ and $\theta_E \approx 55$ K, in reasonably good agreement with the room-temperature value from single-crystal x-ray diffraction.

IV. DISCUSSION

From these measurements, we conclude that $PrRu_4As_{12}$ is a typical paramagnetic metal for which CEF effects play an important role. We find a high-T Pr moment $\mu_{eff} = 3.52$ μ_B from $\chi(T)$ measurements, which is close to the Pr^{3+} free ion value of 3.58 μ_B. The electrical resistivity $\rho(T)$ decreases monotonically with decreasing T, consistent with a simple model that includes impurity/defect, lattice, and s-d scattering processes. Below T_c, we find an excellent example of a BCS superconductor. For comparison purposes, we point out that recent measurements on polycrystalline $PrRu_4As_{12}$ yielded similar superconducting transition temperature values, $T_c = 2.33$ K and $T_c = 2.4$ K.[10,30] Perhaps not surprisingly, we do not see several features that Namiki *et al.* find including, (1) the strong upturn in $C(T)/T$ at low temperatures $T \lesssim 2$ K and (2) the feature at 6 K. As Namiki *et al.* explain, they find an impurity phase in x-ray diffraction data and speculate that the 6 K feature is due to this phase. The low-temperature upturn and the large differences found for $\Delta C(T_c)/\gamma T_c$ may also be due to an impurity phase.

In order to put $PrRu_4As_{12}$ in context, it is informative to reflect on the richness of the behavior found in the Pr-based filled skutterudite compounds, as is most apparent in the first Pr-based heavy-fermion superconductor, $PrOs_4Sb_{12}$.[31–35] This compound enters an unconventional superconducting state at $T_c = 1.85$ K where heavy quasiparticles participate in the formation of Cooper pairs.[33,34,36–41] Upon suppression of the superconductivity with applied magnetic field, an antiferroquadrupolar (AFQ) state is observed for $4.5 \lesssim H \lesssim 16$ T and for $T \lesssim 1$ K, suggesting that the superconductivity may be mediated by AFQ fluctuations.[42,43] In contrast to $PrOs_4Sb_{12}$, the remaining Pr-based filled skutterudites exhibit a variety of ground states including magnetic ordering ($PrFe_4As_{12}$ and $PrOs_4As_{12}$), AFQ ordering ($PrFe_4P_{12}$), conventional superconductivity ($PrRu_4As_{12}$ and $PrRu_4Sb_{12}$), heavy-fermion behavior ($PrFe_4P_{12}$, $PrOs_4As_{12}$, and $PrOs_4Sb_{12}$), metal-insulator transition ($PrRu_4P_{12}$), etc.[5]

Commensurate with the variety of phenomena in these compounds are a large number of CEF level arrangements, which vary unexpectedly from one compound to the next. While $PrRu_4As_{12}$ has a Γ_1 singlet ground state with a Γ_4 first excited state, the other two members of the arsenide series appear to be the reverse of this and have a Γ_5 triplet ground state with a Γ_1 singlet first excited state. This $\Gamma_5 \rightarrow \Gamma_1$ to $\Gamma_1 \rightarrow \Gamma_4$ to $\Gamma_5 \rightarrow \Gamma_1$ evolution of the CEF ground states as $Fe \rightarrow Ru \rightarrow Os$, is not universal in the Pr-based filled skutterudites. For the case of the antimonides, the $\Gamma_5 \rightarrow \Gamma_1$ of $Pr_{1-x}Fe_4Sb_{12}$ becomes $\Gamma_1 \rightarrow \Gamma_5$ for both $PrRu_4Sb_{12}$ and $PrOs_4Sb_{12}$. On the other hand, the lattice parameter behaves as expected; $PrOs_4Sb_{12}$ has the largest value of a of 9.3050 Å and a decreases as the pnictogen or transition-metal ion decreases in size. It is also interesting to note that while $PrOs_4Sb_{12}$ has a small CEF splitting ~7 K between the ground state and first excited state, both $PrRu_4As_{12}$ and $PrRu_4Sb_{12}$ have much larger splittings, ~95 K and ~53 K, respectively. This result may support the notion that the unconventional superconductivity observed in $PrOs_4Sb_{12}$ is related to the small splitting between the ground state and the first excited state. More generally, it seems likely that the ground state for each Pr-based filled skutterudites arises as the result of a delicate balance between several competing factors, among which CEF splitting plays a pivotal role.

V. CONCLUSION

From measurements of magnetization, specific heat, electrical resistivity, and thermopower, $PrRu_4As_{12}$ is found to be a conventional superconductor with a superconducting transition temperature $T_c \approx 2.5$ K. Magnetization measurements indicate that the $4f$ electrons of the Pr ion are localized with $\mu_{eff} = 3.52$ μ_B at high temperatures. From electrical-resistivity measurements, we find conventional metallic behavior above T_c. Specific-heat measurements reveal a mod-

erately large electronic specific-heat coefficient $\gamma \sim 70$ mJ/mol K^2 and that the Pr^{3+} ninefold Hund's rule multiplet is split by the CEF (with a Γ_1 ground state and a Γ_4 first excited state at ~95 K), and that an Einstein mode with a characteristic temperature $\theta_E \approx 55$ K apparently arises from the rattling of the Pr ions in the As atomic cages.

ACKNOWLEDGMENTS

Research at UCSD was supported by the U.S. Department of Energy (Grant No. DE-FG02-04ER46105). Research at ILTSR, Wroclaw was supported by the Polish Ministry of Science and Higher Education (Grant No. N N202 4129 33).

[1] M. B. Maple, E. D. Bauer, N. A. Frederick, P.-C. Ho, W. M. Yuhasz, and V. S. Zapf, Physica B **328**, 29 (2003).
[2] Y. Aoki, H. Sugawara, H. Harima, and H. Sato, J. Phys. Soc. Jpn. **74**, 209 (2005).
[3] M. B. Maple, Z. Henkie, W. M. Yuhasz, P.-C. Ho, T. Yanagisawa, T. A. Sayles, N. P. Butch, J. R. Jeffries, and A. Pietraszko, J. Magn. Magn. Mater. **310**, 182 (2007).
[4] H. Sato, D. Kikuchi, K. Tanaka, M. Ueda, H. Aoki, T. Ikeno, S. Tatsuoka, K. Kuwahara, Y. Aoki, M. Koghi, H. Sugawara, K. Iwasa, and H. Harima, J. Phys. Soc. Jpn. **77** Suppl. A, 1 (2008).
[5] M. B. Maple, Z. Henkie, R. E. Baumbach, T. A. Sayles, N. P. Butch, P.-C. Ho, T. Yanagisawa, W. M. Yuhasz, R. Wawryk, T. Cichorek, and A. Pietraszko, J. Phys. Soc. Jpn. **77** Suppl. A, 7 (2008).
[6] Z. Henkie, M. B. Maple, A. Pietraszko, R. Wawryk, T. Cichorek, R. E. Baumbach, W. M. Yuhasz, and P.-C. Ho, J. Phys. Soc. Jpn. **77** Suppl. A, 128 (2008).
[7] G. M. Sheldrick, *Program for the Solution of Crystal Structures* (University of Göttingen, Germany, 1985).
[8] G. M. Sheldrick, *Program for Crystal Structure Refinement* (University of Göttingen, Germany, 1987).
[9] R. Wawryk and Z. Henkie, Philos. Mag. B **81**, 223 (2001).
[10] T. Namiki, Y. Aoki, H. Sato, C. Sekine, I. Shirotani, T. D. Matsuda, Y. Haga, and T. Yagi, J. Phys. Soc. Jpn. **76**, 093704 (2007).
[11] A. M. Clogston, Phys. Rev. Lett. **9**, 266 (1962).
[12] B. S. Chandrasekhar, Appl. Phys. Lett. **1**, 7 (1962).
[13] N. R. Werthamer, E. Helfand, and P. C. Hohenberg, Phys. Rev. **147**, 295 (1966).
[14] *Physical Properties of Superconductors*, edited by D. M. Ginsberg (World Scientific, Singapore, 1989), Chap. 2.
[15] M. Tinkham, *Introduction to Superconductivity* (McGraw-Hill, New York, 1975).
[16] P.-C. Ho, N. P. Butch, V. S. Zapf, T. Yanagisawa, N. A. Frederick, S. K. Kim, W. M. Yuhasz, M. B. Maple, J. B. Betts, and A. H. Lacerda, J. Phys.: Condens. Matter **20**, 215226 (2008).
[17] N. A. Frederick, T. A. Sayles, and M. B. Maple, Phys. Rev. B **71**, 064508 (2005).
[18] G. W. Webb, Phys. Rev. **181**, 1127 (1969).
[19] Z. Kletowski, R. Fabrowski, P. Slawinski, and Z. Henkie, J. Magn. Magn. Mater. **166**, 361 (1997).
[20] N. F. Mott and H. Jones, *The Theory of the Properties of Metals and Alloys* (Oxford University Press, Oxford, 1936).
[21] F. J. Blatt, P. A. Schroeder, C. L. Foiles, and D. Greig, *Thermoelectric Power of Metals* (Plenum Press, New York, London, 1976), p. 147.
[22] K. Behnia, D. Jaccard, and J. Flouquet, J. Phys.: Condens. Matter **16**, 5187 (2004).
[23] V. Zlatić, R. Monnier, J. K. Freericks, and K. W. Becker, Phys. Rev. B **76**, 085122 (2007).
[24] K. R. Lea, M. J. M. Leask, and W. P. Wolf, J. Phys. Chem. Solids **23**, 1381 (1962).
[25] K. Takegahara, H. Harima, and A. Yanase, J. Phys. Soc. Jpn. **70**, 1190 (2001).
[26] E. A. Goremychkin, R. Osborn, E. D. Bauer, M. B. Maple, N. A. Frederick, W. M. Yuhasz, F. M. Woodward, and J. W. Lynn, Phys. Rev. Lett. **93**, 157003 (2004).
[27] N. H. Andersen, P. E. Gregers-Hansen, E. Holm, H. Smith, and O. Vogt, Phys. Rev. Lett. **32**, 1321 (1974).
[28] B. C. Sales, B. C. Chakoumakos, D. Mandrus, J. W. Sharp, N. R. Dilley, and M. B. Maple, *Materials Research Society 1998 Fall Proceedings, Symposium Z, Thermoelectric Materials: The Generation of Materials for Small Scale Refrigeration and Power Generation Applications*, MRS Symposia Proceedings No. 545 (Materials Research Society, Pittsburgh, 1999), p. 13.
[29] P.-C. Ho, W. M. Yuhasz, N. P. Butch, N. A. Frederick, T. A. Sayles, J. R. Jeffries, M. B. Maple, J. B. Betts, A. H. Lacerda, P. Rogl, and G. Giester, Phys. Rev. B **72**, 094410 (2005).
[30] I. Shirotani, T. Uchiumi, K. Ohno, C. Sekine, Y. Nakazawa, K. Kanoda, S. Todo, and T. Yagi, Phys. Rev. B **56**, 7866 (1997).
[31] M. B. Maple, E. D. Bauer, V. S. Zapf, E. J. Freeman, N. A. Frederick, and R. P. Dickey, Acta Phys. Pol. B **32**, 3291 (2001).
[32] E. D. Bauer, N. A. Frederick, P.-C. Ho, V. S. Zapf, and M. B. Maple, Phys. Rev. B **65**, 100506 (2002).
[33] N. Nakai, M. Ichioka, and K. Machida, J. Phys. Soc. Jpn. **71**, 23 (2002).
[34] M. B. Maple, N. A. Frederick, P. C. Ho, W. M. Yuhasz, and T. Yanagisawa, J. Supercond. Novel Magn. **19**, 299 (2006).
[35] B. Andraka, C. R. Rotundu, and K. Ingersent, Phys. Rev. B **81**, 054509 (2010).
[36] K. Izawa, Y. Nakajima, J. Goryo, Y. Matsuda, S. Osaki, H. Sugawara, H. Sato, P. Thalmeier, and K. Maki, Phys. Rev. Lett. **90**, 117001 (2003).
[37] R. W. Hill, S. Li, M. B. Maple, and L. Taillefer, Phys. Rev. Lett. **101**, 237005 (2008).
[38] G. Seyfarth, J. P. Brison, M. A. Measson, D. Braithwaite, G. Lapertot, and J. Flouquet, Phys. Rev. Lett. **97**, 236403 (2006).
[39] L. Shu, D. E. MacLaughlin, W. P. Beyermann, R. H. Heffner, G. D. Morris, O. O. Bernal, F. D. Callaghan, J. E. Sonier, W. M. Yuhasz, N. A. Frederick, and M. B. Maple, Phys. Rev. B **79**, 174511 (2009).
[40] T. Cichorek, A. C. Mota, F. Steglich, N. A. Frederick, W. M. Yuhasz, and M. B. Maple, Phys. Rev. Lett. **94**, 107002 (2005).
[41] Y. Aoki, A. Tsuchiya, T. Kanayama, S. R. Saha, H. Sugawara, H. Sato, W. Higemoto, A. Koda, K. Ohishi, K. Nishiyama, and R. Kadono, Phys. Rev. Lett. **91**, 067003 (2003).
[42] P.-C. Ho, N. A. Frederick, V. S. Zapf, E. D. Bauer, T. D. Do, M. B. Maple, A. D. Christianson, and A. H. Lacerda, Phys. Rev. B **67**, 180508(R) (2003).
[43] M. Kohgi, K. Iwasa, M. Nakajima, N. Metoki, S. Araki, N. Bernhoeft, J. M. Mignot, A. Gukasov, H. Sato, Y. Aoki, and H. Sugawara, J. Phys. Soc. Jpn. **72**, 1002 (2003).